Microstructure of vinylidene cyanide copolymers with linear-chain fatty acid vinyl esters

Yoshihisa Ohta, Yoshio Inoue* and Riichiro Chûjô
Department of Biomolecular Engineering, Tokyo Institute of Technology, 0-okayama 2-chome, Meguro-ku, Tokyo 152, Japan

and Manabu Kishimoto and Iwao Seo
Mitsubishi Petrochemical Co. Ltd., 8-3-1 Chuo, Ami-machi, Inashiki-gun, Ibaraki 300-03, Japan
(Received 29 June 1989; revised 22 September 1989; accepted 28 September 1989)

The microstructure of vinylidene cyanide (VDCN) copolymers with linear-chain fatty acid vinyl esters, vinyl propionate, vinyl butyrate and vinyl hexanoate, was studied by 67.9 MHz ^{13}C n.m.r. spectroscopy. It was found that the compositional sequence distributions obtained from the analysis of the cyanide carbon (VDCN-centred) pentad and the methine carbon (comonomer-centred) triad resonances of all copolymers were highly alternative. Tactic structures in the alternating sequence were almost completely atactic. The microstructures of all copolymers were not largely different from each other. So, we suppose that possible origins of piezoelectricity observed for vinylidene cyanide copolymers should be found in other factors than the microstructure.

(Keywords: poly(vinylidene cyanide-co-linear-chain fatty acid vinyl ester); ^{13}C n.m.r.; compositional sequence distribution; tacticity; microstructure; piezoelectricity)

INTRODUCTION

In 1980, Miyata *et al.*[1] found large piezoelectricity in poly(vinylidene cyanide-co-vinyl acetate) [P(VDCN/VAc)]. This copolymer is amorphous and its film shows fairly high piezoelectric activity after drawing and poling treatments.

Before the discovery of piezoelectricity in this copolymer, some piezoelectric polymers, such as poly(vinylidene fluoride) and poly(vinylidene fluoride-co-trifluoroethylene), were known and molecular origin of their piezoelectric activity has been studied[2–7]. The fluoropolymers show larger piezoelectricity than the cyanide copolymers. One of the significant differences between these polymers is found in the morphology. The piezoelectric fluoropolymers are crystalline, but the cyanide copolymer is amorphous. The film of the amorphous polymer has better transparency and flexibility than that of the crystalline ones. The amorphous cyanide copolymer has higher thermostability than the crystalline fluoropolymers, for example, the decomposition temperature of P(VDCN/VAc) is about 160°C, whereas that of PVDF is about 80–100°C[8].

It is undoubted that the piezoelectric activity of P(VDCN/VAc) is caused by the side-chain C–C≡N dipoles. The piezoelectric activity comparable to that of P(VDCN/VAc) is expected for poly(vinylidene cyanide-co-methyl methacrylate) (P(VDCN/MMA)) and poly(vinylidene cyanide-co-styrene) (P(VDCN/St)) because the C–C≡N dipoles are also present in these copolymers. But the piezoelectric d_{31} constants of P(VDCN/MMA) and P(VDCN/St) are only 0.4 and 0.2 pC N^{-1}, which amounts to about one tenth and one twentieth of that of P(VDCN/VAc)[8,9]. These results suggest that there are other possible origins of high piezoelectricity in the cyanide copolymers.

Recently, the microstructures of P(VDCN/VAc), P(VDCN/MMA), P(VDCN/St), poly(vinylidene cyanide-co-vinyl benzoate) [P(VDCN/VBz)] and poly(vinylidene cyanide-co-vinyl pivalate) [P(VDCN/VPiv)] have been analysed successfully by ^{13}C n.m.r. spectroscopy[11–14]. It was found that their microstructures did not differ greatly from each other. Both high and low piezoelectric polymers have highly alternating and configurationally random sequences. The configurational randomness can explain the amorphous character of these copolymers, but the information on the microstructure of only a few polymers is not enough to explain the molecular origin of piezoelectric activity of the VDCN copolymers.

In this paper, the primary structures such as monomer composition, monomer sequence distribution, and tacticity of vinylidene cyanide copolymers with linear-chain fatty acid vinyl esters; poly(vinylidene cyanide-co-vinyl propionate) [P(VDCN/VPr)], poly(vinylidene cyanide-co-vinyl butylate) [P(VDCN/VBu)], and poly(vinylidene cyanide-co-vinyl hexanoate) [P(VDCN/VHe)], are determined and compared with each other on the basis of ^{13}C n.m.r. analyses. The piezoelectric strain constants d_{31} of these copolymers, which were poled at temperatures 10°C below the glass transition temperatures and under an electric field strength of 450 kV cm^{-1} for 2 h, are about 3.0 pC N^{-1} (ref. 9). The origin of the piezoelectricity in these copolymers will be briefly discussed.

* To whom correspondence should be addressed

0032-3861/90/081581-08

EXPERIMENTAL

Materials

The details of general procedures for the preparation of VDCN copolymers have been reported elsewhere[11]. The copolymers of VDCN with VPr, VBu and VHe were synthesized by radical polymerization at 70°C. Lauroyl peroxide [LPO] was used as the initiator.

N.m.r. measurements

^{13}C n.m.r. spectra were measured by using a Jeol GX-270 high-resolution spectrometer at 67.9 and 100 MHz in solutions of perdeuterated dimethyl sulphoxide [DMSO-d_6] with sample concentrations of 7.9–11 wt%. The sample solutions were contained in 10 mm o.d. glass tubes. The spectral data points were 64 000. A pulse angle of 45° and a pulse repetition time of 10 s were chosen. FT spectra of P(VDCN/VPr), P(VDCN/VBu) and P(VDCN/VHe) were obtained after accumulation of 25 118, 20 606, and 16 427 interferograms, respectively. The peak resolution and the estimation of relative peak intensity were made by using a curve resolution program [CRP][15].

RESULTS AND DISCUSSION

Figure 1 shows the 67.9 MHz ^{13}C n.m.r. spectrum of P(VDCN/VHe) in DMSO-d_6 at 100°C. Each peak is very sharp and simple, and the assignments were made by comparison with the spectrum of P(VDCN/VAc)[11]. We conclude that the monomeric units of VDCN, VPr, VBu, and VHe are almost all arranged in head-to-tail fashion and most monomer sequences are alternating. The assignments are summarized in *Table 1*. Similarly, the spectra of P(VDCN/VPr) and P(VDCN/VBu) shown in *Figures 2* and *3* were assigned and the results are summarized in *Tables 2* and *3*, respectively.

Copolymer sequence structure

Figure 4 shows the expanded resonance for the cyanide carbon region of P(VDCN/VHe). In this region, there are strong triplet peaks (A), (B) and (C), and two groups of some weak peaks (D) and (E). *Figure 4* also shows the peak resolution obtained by using CRP. Each peak that was observed for the cyanide carbon in the VDCN unit was assigned to one of compositional pentads. In the previous papers[11–14], it has been found that the vinylidene cyanide copolymers were highly alternating. Thus, the three main split peaks in *Figure 4* were supposed to assign the (VDCN–VHe–VDCN–VHe–VDCN) pentad structure and the four weak resonances (D) to the (VDCN–VHe–VDCN–VDCN–VHe) pentad and is the next highly probable pentad sequence. Considering the tacticity, the peak number does not conflict.

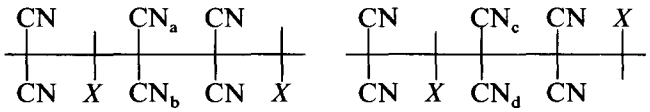

X represents VPr, VBu and VHe unit.

Moreover, the weak peaks (E) were assigned to the (VDCN–VHe–VDCN—VHe–VHe) pentad because for this pentad there are eight kinds of magnetically non-equivalent cyanide carbons with the same probability (*Figure 4*).

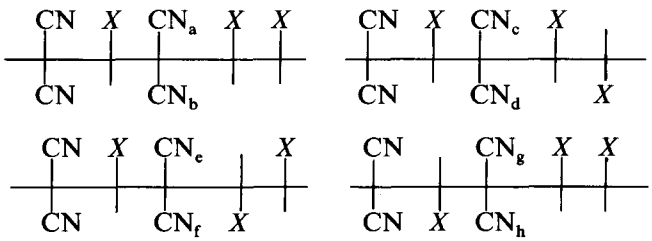

X represents VPr, VBu and VHe unit.

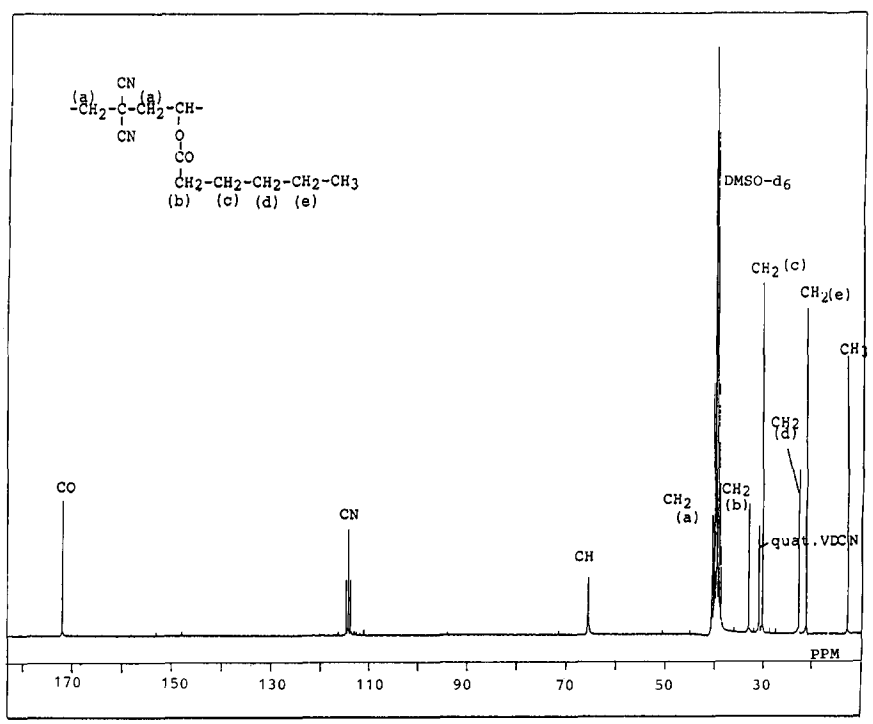

Figure 1 67.9 MHz ^{13}C n.m.r. spectrum of P(VDCN/VHe) observed in 7.9% (w/v) DMSO-d_6 solution at 100°C

Table 1 Chemical shift assignments of P(VDCN/VHe)

Carbon	Chemical shift (ppm)	Assignments
CO	171.98	VDCN–VHe–VDCN
CN	114.63, 114.17, 113.73	VHe–VDCN–VHe
	113.01, 112.93, 112.56, 112.49	VDCN–VDCN–VHe
CH	65.70, 65.50, 65.31	VDCN–VHe–VDCN
	65.63, 65.60, 65.42, 65.38	VHe–VHe–VDCN
CH_2(a)	40.49	VDCN–VHe
CH_2 VHe(b)	32.86	VDCN–VHe–VDCN
Quaternary VDCN	30.80–30.71	VDCN–VHe–VDCN
CH_2 VHe(c)	30.00	VDCN–VHe–VDCN
CH_2 VHe(d)	22.59–22.56	VDCN–VHe–VDCN
CH_2 VHe(e)	21.01	VDCN–VHe–VDCN
CH_3	12.84	VDCN–VHe–VDCN

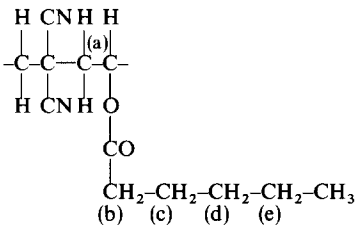

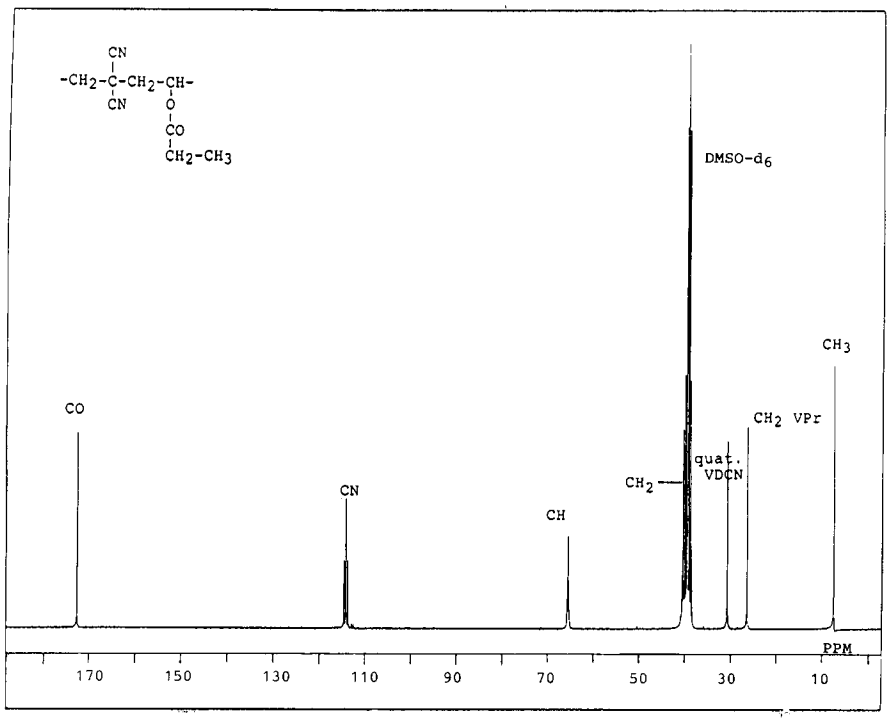

Figure 2 67.9 MHz ^{13}C n.m.r. spectrum of P(VDCN/VPr) observed in 11.0% (w/v) DMSO-d_6 solution at 100°C

The three splits in the main VDCN-centred cyanide resonance originate from the effect of tacticity as will be discussed later. However, no peak corresponding to the other compositional pentads were observed because the VDCN homosequence may be subject to a chain scission reaction by atmospheric moisture at room temperature[16].

From the compositional results with respect to the VDCN-centred pentads, we can calculate the conditional probability P_{12} that a VDCN–VHe unit comes about as a result of a VDCN growing chain end adding to VHe, as follows:

$$P_{12} = \frac{\begin{array}{c}(\text{VDCN–VHe–VDCN–VHe–VDCN}) \\ +(\text{VDCN–VHe–VDCN–VHe–VHe}) \\ +(\text{VDCN–VHe–VDCN–VDCN–VHe})/2\end{array}}{\sum(\text{VDCN-centroid pentad sequences})}$$

The compositional information concerning the VHe-centred triads can be obtained from the resonance region of VHe methine carbon. *Figure 5* shows the expanded resonance of the methine carbon region. There are three

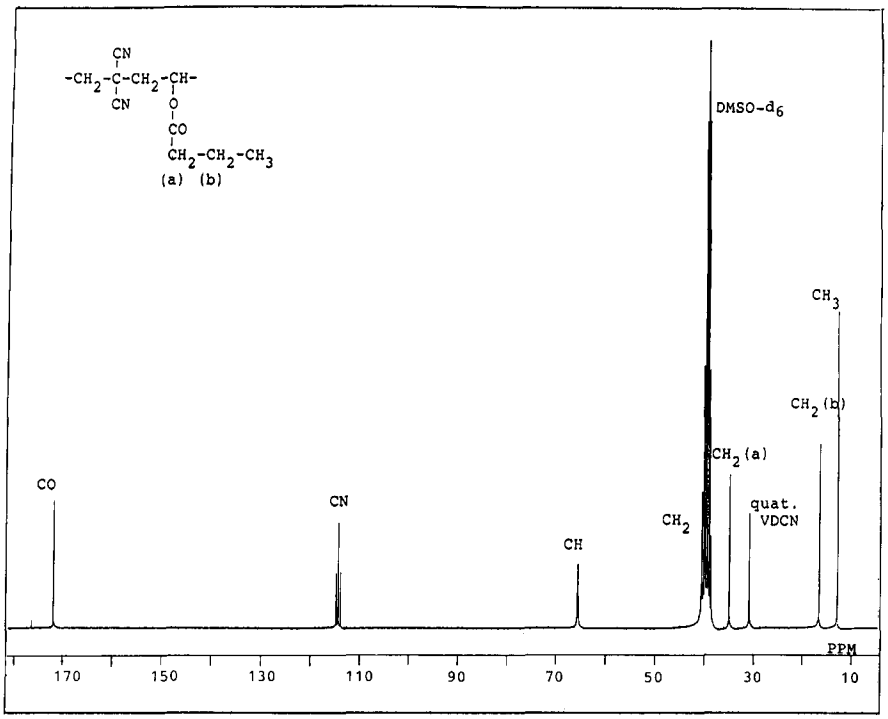

Figure 3 67.9 MHz ^{13}C n.m.r. spectrum of P(VDCN/VBu) observed in 8.4% (w/v) DMSO-d_6 solution at 100°C

Table 2 Chemical shift assignments of P(VDCN/VPr)

Carbon	Chemical shift (ppm)	Assignments
CO	172.75	VDCN–VPr–VDCN
CN	114.59, 114.17, 113.76	VPr–VDCN–VPr
	113.00, 112.93, 112.59, 112.52	VDCN–VDCN–VPr
CH	65.73, 65.55, 65.37	VDCN–VPr–VDCN
CH_2	40.51–40.48	VDCN–VPr
Quaternary VDCN	30.80–30.55	VDCN–VPr–VDCN
CH_2 VPr	26.50	VDCN–VPr–VDCN
CH_3	7.49	VDCN–VPr–VDCN

Table 3 Chemical shift assignments of P(VDCN/VBu)

Carbon	Chemical shift (ppm)	Assignments
CO	171.85	VDCN–VBu–VDCN
CN	114.63, 114.18, 113.75	VBu–VDCN–VBu
	113.01, 112.93, 112.57, 112.49	VDCN–VDCN–VBu
CH	65.69, 65.50, 65.33	VDCN–VBu–VDCN
	65.63, 65.59, 65.41, 65.26	VBu–VBu–VDCN
CH_2	40.53, 40.58	VDCN–VBu
CH_2 VBu(a)	34.86	VDCN–VBu–VDCN
Quaternary VDCN	30.82–30.73	VDCN–VBu–VDCN
CH_2 VBu(b)	16.46–16.35	VDCN–VBu–VDCN
CH_3	12.72	VDCN–VBu–VDCN

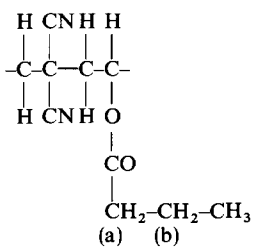

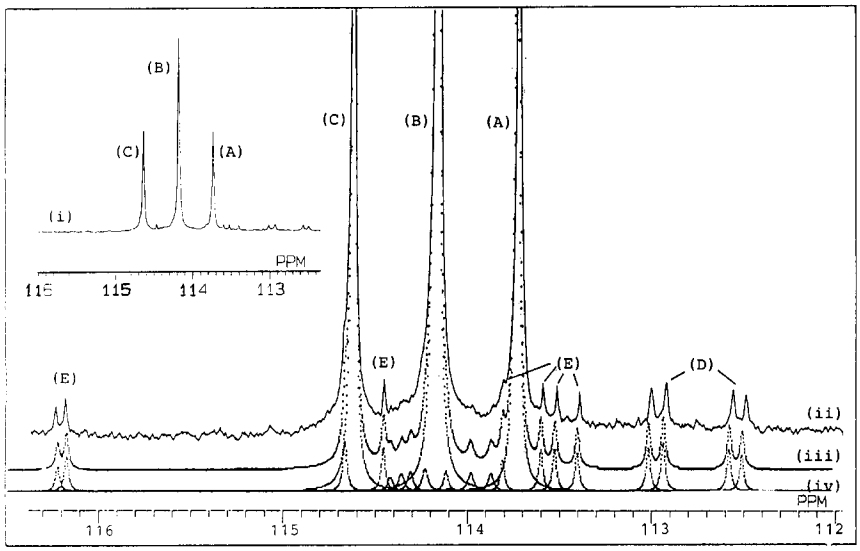

Figure 4 Spectrum of the cyanide carbon resonance region of P(VDCN/VHe). Curve (i) observed spectrum; curve (ii) expanded spectrum; curve (iii) reproduced spectrum from resolved components; curve (iv) results of curve resolution. Labelling of peaks is explained in the text

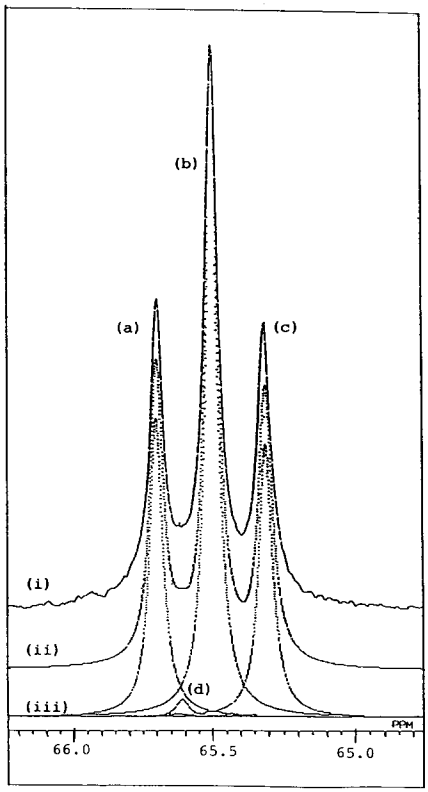

Figure 5 Spectrum of the methine carbon resonance region of P(VDCN/VHe). Curve (i) observed spectrum; curve (ii) reproduced spectrum from resolved components; curve (iii) results of curve resolution. Labelling of peaks is explained in the text

main peaks (a, b and c) and some weak peaks (d) at the tail of the main peaks. These peaks were resolved by using CRP as shown in *Figure 5*. With respect to the compositional triad, similar to VDCN-centred pentads, the main peaks (a, b and c) can be assigned to the (VDCN–VHe–VDCN) triad. Small peaks (d) were assigned to the (VDCN–VHe–VHe) triad which is the next highly probable sequence. The VHe homotriad was considered to be negligible.

It is the first time that the cyanide carbon spectra were assigned with respect to the compositional pentad for the VDCN-centred sequence. We cannot still understand the reasons why the resolution of the cyanide carbon spectra of the copolymers investigated in this paper is high, but suggest that ^{13}C spectra shown here and those in the previous papers were observed at different n.m.r. frequencies, i.e., 67.9 JHz and 125 MHz, respectively.

In the same way as reported in previous papers[11], we calculate the conditional probability P_{21} representing that the VDCN growing chain end will add VHe unit to give the sequence of VDCN–VHe:

$$P_{21}=\frac{(\text{VDCN–VHe—VDCN})+(\text{VDCN–VHe–VHe})/2}{(\text{VDCN–VHe–VDCN})+(\text{VDCN–VHe–VHe})+(\text{VHe–VHe–VHe})}$$

The values of P_{12} and P_{21} are given in *Table 4* with those of P(VDCN/VPr) and P(VDCN/VBu) calculated in the same way. The expanded spectra of P(VDCN/VPr) and P(VDCN/VBu) are shown in *Figures 6* and *7*. The spectra similar with those of P(VDCN/VHe) were observed.

Further, the compositions of three possible dyad sequences and the monomer compositions can be also estimated by using the pentad and triad compositional distributions. The values of dyad and monomer compositions are also given in *Table 4*. From the fact that the values of P_{12} and P_{21} are nearly 1, and monomer composition ratios are actually 1:1, we deduce that the three copolymers have highly alternating character. These results can be explained by the Q–e concept. As the Q value of VDCN monomer is 20.13, it is known to be the highly conjugated monomer[17]. Furthermore, VDCN is an electron-accepting monomer because the e value is 2.58 so that the electron density on the part of double bond is extremely deteriorated[17]. From these facts, VDCN monomer is more reactive with the highly reactive vinyl ester radicals than vinyl ester monomer is, while vinyl ester monomer is more reactive than VDCN monomer toward the VDCN radical. Thus, the results that the VDCN–vinyl ester copolymers show highly alternating characters are consistent with this expectation.

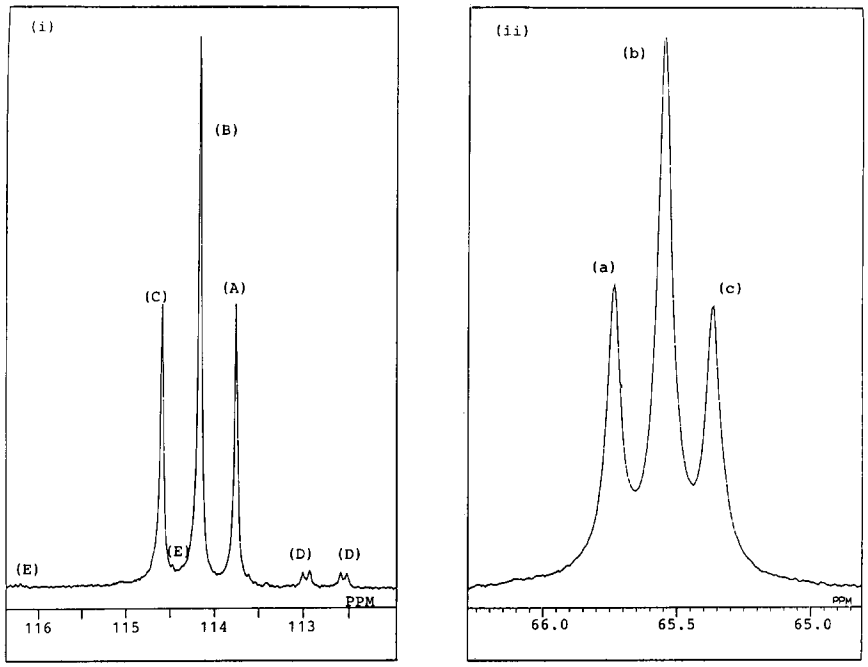

Figure 6 Expanded spectra of P(VDCN/VPr). (i) The cyanide carbon resonance region; (ii) the methine carbon resonance region

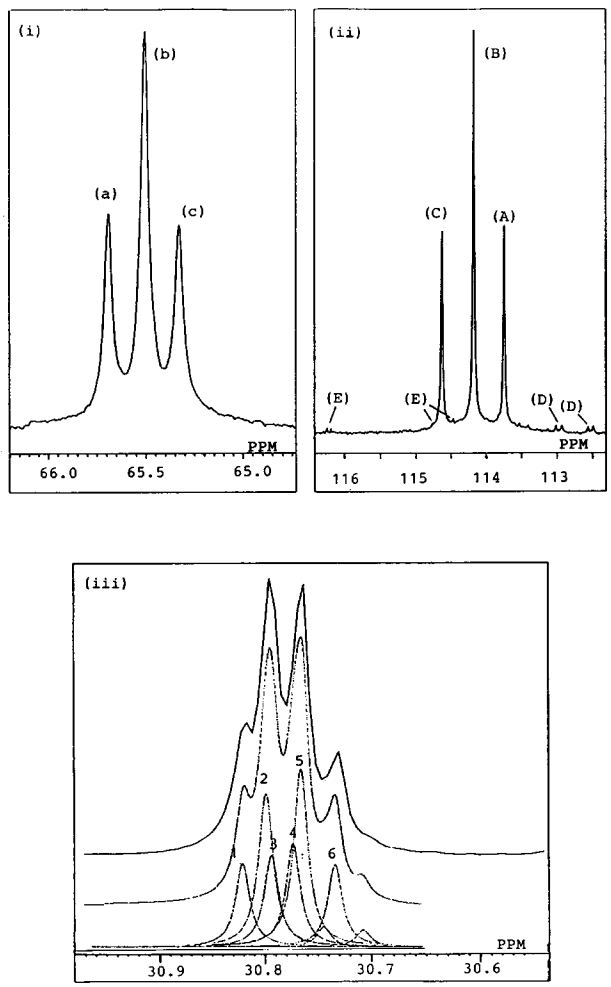

Figure 7 Expanded spectra of P(VDCN/VBu). (i) The methine carbon resonance region; (ii) the cyanide carbon resonance region; (iii) the backbone quaternary carbon resonance region, including the calculated spectrum by CRP. Peak 1, $r_\varepsilon m_\varepsilon r_\varepsilon$; peak 2, $r_\varepsilon r_\varepsilon m_\varepsilon + m_\varepsilon r_\varepsilon r_\varepsilon$; peak 3, $m_\varepsilon r_\varepsilon m_\varepsilon$; peak 4, $m_\varepsilon m_\varepsilon m_\varepsilon$; peak 5, $m_\varepsilon m_\varepsilon r_\varepsilon + r_\varepsilon m_\varepsilon m_\varepsilon$; peak 6, $r_\varepsilon r_\varepsilon r_\varepsilon$. m_ε and r_ε are defined in the text

Table 4 Copolymerization parameters in VDCN–VPr, VDCN–VBu and VDCN–VHe systems determined from cyanide and the methine carbon resonances

Parameter	P(VDCN/VPr)	P(VDCN/VBu)	P(VDCN/VHe)
P_{12}	0.976	0.983	0.975
P_{21}	0.987	0.990	0.991
(VDCN–VDCN)	0.012	0.009	0.013
(VDCN–*X*)[a]	0.985	0.989	0.985
(*X*–*X*)	0.003	0.002	0.002
VDCN	0.505	0.503	0.505
X	0.495	0.497	0.495

[a] *X* represents VPr, VBu and VHe units

Configurational structure

In order to analyse the tactic structure of alternating copolymer, the concept of ε-tacticity defined by Jo *et al.*[11] is useful. As the copolymers have highly alternating characters, we assume the VDCN–*X* dyad as the repeating unit in the alternating sequence. Two configurationally different structures in the dyad sense are possible:

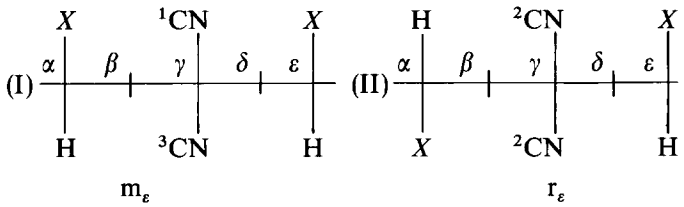

where *X* is $-OCOC_2H_5$ for P(VDCN/VPr), $-OCOC_3H_7$ for P(VDCN/VBu), and $-OCOC_5H_{11}$ for P(VDCN/VHe). Here, the configurations of the chains in formulae I and II are defined as ε-isotactic and ε-syndiotactic, respectively. The relative tactic enchainments in formulae I and II are defined as m_ε (ε-meso) and r_ε (ε-racemo), respectively. As described earlier in *Figure 4*, splitting of the cyanide carbon resonance of the (VDCN–VHe–VDCN–VHe–VDCN) pentad into three main peaks (A), (B) and (C),

is caused by the ε-tactic arrangement. Because the cyanide carbons (1) and (3) are magnetically non-equivalent while the carbons (2) are magnetically equivalent, the appearance of three peaks in the cyanide carbon resonance is reasonable. Three peaks, (A), (B) and (C), are assigned to the carbons denoted by (1), (2) and (3) in formulae I and II, respectively. Although the assignments of (1) and (3) carbons are not yet clearly verified, it is considered that the resonance of carbon (1) appears at the higher field region than that of (3), which may be a similar situation to the case of the carbonyl carbon resonance of styrene–methyl methacrylate copolymer, where the co-isotactic peak has been assigned at higher field than the co-syndiotactic peak[18,19]. Apparently, the peak at intermediate field is assigned as the resonance of carbons (2).

The ε-isotactic probability σ_ε is calculated from the following equation:

$$\sigma_\varepsilon = ([A]+[C])/([A]+[B]+[C])$$

where $[A]$, $[B]$ and $[C]$ are the relative intensities of the corresponding cyanide carbon resonances estimated by using CRP. The σ_ε values obtained for P(VDCN/VPr), P(VDCN/VBu), and P(VDCN/VHe) are 0.510, 0.507 and 0.511, respectively, indicating that these copolymers are completely atactic. This result explains why these copolymers are amorphous in the solid state. As shown in *Figure 4*, the methine carbon resonances are split into three peaks (a), (b) and (c), due to ε-tactic triad in the alternating sequence. Each peak arises from ε-tacticity, namely ε-syndiotactic ($r_\varepsilon r_\varepsilon$), ε-heterotactic ($m_\varepsilon r_\varepsilon + r_\varepsilon m_\varepsilon$) and ε-isotactic ($m_\varepsilon m_\varepsilon$). The peak appeared at intermediate field (b) is evidently assigned to ε-heterotactic, while we cannot easily know the assignments of the other two peaks (a) and (c). If one assumes a terminal Bernoullian control model with a single parameter σ_ε as a stereospecific polymerization mechanism, ε-tactic probability ratio is expressed as follows,

$$(1-\sigma_\varepsilon)^2 : 2\sigma_\varepsilon(1-\sigma_\varepsilon) : \sigma_\varepsilon^2$$

By using the σ_ε values determined by cyanide carbon resonances, the ratios are estimated as shown in *Tables 5*, *6* and *7*, together with the relative peak intensities obtained experimentally by CRP. By comparison of the observed ratios with the calculated ones, the two peaks (a) and (c) are assigned to $m_\varepsilon m_\varepsilon$ and $r_\varepsilon r_\varepsilon$, respectively.

Figure 8 shows the expanded resonance for the backbone quaternary carbon region of P(VDCN/VHe), indicating some peaks possibility due to ε-tactic tetrads. Though the low digital resolution of the spectrum makes the edges in the peaks, we can recognize the described tendency of the splits for tetrads. This resonance was also

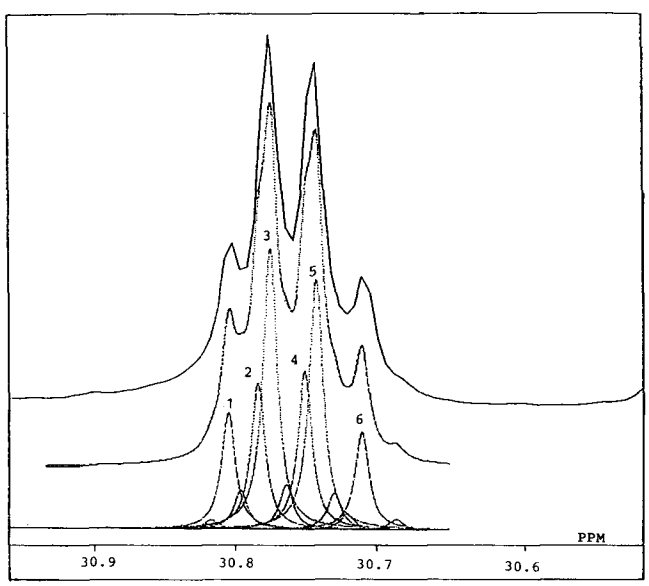

Figure 8 Expanded spectrum of the backbone quaternary carbon resonance region of P(VDCN/VHe), including the calculated spectrum by CRP. Peak 1, $r_\varepsilon m_\varepsilon r_\varepsilon$; peak 2, $m_\varepsilon r_\varepsilon m_\varepsilon$; peak 3, $m_\varepsilon m_\varepsilon r_\varepsilon + r_\varepsilon m_\varepsilon m_\varepsilon$; peak 4, $m_\varepsilon m_\varepsilon m_\varepsilon$; peak 5, $r_\varepsilon m_\varepsilon m_\varepsilon + m_\varepsilon m_\varepsilon r_\varepsilon$; peak 6, $r_\varepsilon r_\varepsilon r_\varepsilon$

Table 5 Signal assignments and relative intensities in alternating fractions of P(VDCN/VPr)

Carbon	Chemical shift (ppm)	Assignment	Relative intensity: Observed	Relative intensity: Calculated[a]
CN	114.59	ε-isotactic	0.253	–
	114.17	ε-syndiotactic	0.490	–
	113.76	ε-isotactic	0.257	–
CH	65.63	$m_\varepsilon m_\varepsilon$	0.266	0.260
	65.55	$m_\varepsilon r_\varepsilon + r_\varepsilon m_\varepsilon$	0.495	0.500
	65.37	$r_\varepsilon r_\varepsilon$	0.239	0.240

[a] Value calculated on the assumption of Bernoullian statistics probability $\sigma_\varepsilon = 0.510$, which is estimated from the cyanide carbon resonance

Table 6 Signal assignments and relative intensities in alternating fractions of P(VDCN/VBu)

Carbon	Chemical shift (ppm)	Assignment	Relative intensity: Observed	Relative intensity: Calculated[a]
CN	114.63	ε-isotactic	0.249	–
	114.18	ε-syndiotactic	0.493	–
	113.75	ε-isotactic	0.258	–
CH	65.69	$m_\varepsilon m_\varepsilon$	0.262	0.257
	65.50	$m_\varepsilon r_\varepsilon + r_\varepsilon m_\varepsilon$	0.496	0.500
	65.33	$r_\varepsilon r_\varepsilon$	0.242	0.243
Quaternary VDCN	30.82	$r_\varepsilon m_\varepsilon r_\varepsilon$	0.121	0.123
	30.80	$r_\varepsilon r_\varepsilon m_\varepsilon + m_\varepsilon r_\varepsilon r_\varepsilon$	0.221	0.246
	30.79	$m_\varepsilon r_\varepsilon m_\varepsilon$	0.132	0.127
	30.77	$m_\varepsilon m_\varepsilon m_\varepsilon$	0.150	0.130
	30.76	$m_\varepsilon m_\varepsilon r_\varepsilon + r_\varepsilon m_\varepsilon m_\varepsilon$	0.256	0.253
	30.73	$r_\varepsilon r_\varepsilon r_\varepsilon$	0.120	0.120

[a] Value calculated on the assumption of Bernoullian statistics probability $\sigma_\varepsilon = 0.510$, which is estimated from the cyanide carbon resonance

Table 7 Signal assignments and relative intensities in alternating fractions of P(VDCN/VHe)

Carbon	Chemical shift (ppm)	Assignment	Relative intensity: Observed	Relative intensity: Calculated[a]
CN	114.63	ε-isotactic	0.255	–
	114.17	ε-syndiotactic	0.489	–
	113.73	ε-isotactic	0.256	–
CH	65.70	$m_\varepsilon m_\varepsilon$	0.265	0.261
	65.50	$m_\varepsilon r_\varepsilon + r_\varepsilon m_\varepsilon$	0.493	0.493
	65.31	$r_\varepsilon r_\varepsilon$	0.242	0.240
Quaternary VDCN	30.80	$r_\varepsilon m_\varepsilon r_\varepsilon$	0.109	0.122
	30.78	$m_\varepsilon r_\varepsilon m_\varepsilon$	0.142	0.128
	30.77	$m_\varepsilon m_\varepsilon r_\varepsilon + r_\varepsilon m_\varepsilon m_\varepsilon$	0.269	0.255
	30.75	$m_\varepsilon m_\varepsilon m_\varepsilon$	0.153	0.133
	30.74	$r_\varepsilon m_\varepsilon m_\varepsilon + m_\varepsilon m_\varepsilon r_\varepsilon$	0.236	0.244
	30.71	$r_\varepsilon r_\varepsilon r_\varepsilon$	0.091	0.117

[a] Value calculated on the assumption of Bernoullian statistics probability $\sigma_\varepsilon = 0.510$, which is estimated from the cyanide carbon resonance

resolved by using CRP, and six peaks are tentatively assigned on the basis of relative intensities predicted from the Bernoullian statistics, as shown in *Figure 8*. The split of the peak due to the difference in the tactic structure can be seen in the resonance of quaternary carbon for P(VDCN/VBu) (*Figure 7iii*) but cannot be seen in the resonance of that for P(VDCN/VPr). The observed values of tacticity in alternating sequence of P(VDCN/VPr), P(VDCN/VBu) and P(VDCN/VHe) are given in *Tables 5, 6* and *7*, respectively.

CONCLUSION

Monomer composition, comonomer sequence distribution and tactic structure can be determined by ^{13}C n.m.r. spectroscopy for P(VDCN/VPr), P(VDCN/VBu) and P(VDCN/VHe). It becomes apparent that the characteristics of microstructures described above for P(VDCN/VPr), P(VDCN/VBu) and P(VDCN/VHe), and other vinylidene cyanide copolymers reported in the previous papers[11–14] do not differ from each other. The three cyanide copolymers investigated in this paper have highly alternating and configurationally random sequences. From these results, there are no effects of the length of alkyl side-chain on the characteristics of microstructure. Thus, the reason why some vinylidene cyanide copolymers show high piezoelectricity and others do not should be found in other factors than the microstructure.

REFERENCES

1 Miyata, S., Yoshikawa, M., Tasaka, S. and Ko, M. *Polym. J.* 1980, **12**, 857
2 Kawai, H. *Jpn. J. Appl. Phys.* 1969, **8**, 975
3 Furukawa, T., Johnson, G. E., Bair, H. E., Tajitu, Y., Chiba, A. and Fukada, E. *Ferroelectrics* 1981, **32**, 61
4 Yagi, T. and Tatemoto, M. *Polym. J.* 1979, **11**, 429
5 Furukawa, T. and Wen, J. X. *Jpn. J. Appl. Phys.* 1984, 23, L677
6 Tashiro, K., Takano, K., Kobayashi, M., Chatani, Y. and Tadokoro, H. *Polymer* 1982, **22**, 1312
7 Lovinger, A. J., Furukawa, T., Davis, G. T. and Broadhurst, M. G. *Macromolecules* 1983, **16**, 1855
8 Seo, I. and Nakajima, K. *Nikkei New Materials* 1986, Feb. 24, p. 50
9 Kishimoto, M., Fujimoto, Y. and Seo, I. *Polym. Prep. Jpn.* 1989, **38**, 1012
10 Miyata, S., Yoshikawa, M., Tasaka, S. and Ko, M. *Polym. J.* 1986, **12**, 857
11 Jo, Y. S., Inoue, Y., Chûjô, R., Saito, K. and Miyata, S. *Macromolecules* 1985, **18**, 1850
12 Maruyama, Y., Jo, Y. S., Inoue, Y., Chûjô, R., Tasaka, S. and Miyata, S. *Polymer* 1987, **28**, 1583
13 Inoue, Y., Kashiwazaki, A., Maruyama, Y., Jo, Y. S., Chûjô, R., Kishimoto, M. and Seo, I. *Polymer* 1988, **29**, 144
14 Inoue, Y., Kawaguchi, K., Maruyama, Y., Jo, Y. S., Chûjô, R., Kishimoto, M. and Seo, I. *Polymer* 1989, **30**, 698
15 Hayashi, T., Inoue, Y., Chûjô, R. and Asakura, T. *Polymer* 1988, **29**, 138
16 Gilbert, H., Miller, F. F., Averill, S. J., Schmidt, R. F., Stewart, F. D., Trumbull, H. L. *J. Am. Chem. Soc.* 1954, **76**, 1074
17 Yoshida, H. and Kobayashi, Y. *J. Macromol. Sci. Phys.* 1982, **B21**, 565
18 Hirai, H., Koinuma, H., Tanabe, T. and Takeuchi, K. *J. Polym. Sci., Polym. Chem. Edn.* 1979, **17**, 1339
19 Ebdon, J. R., Huckerby, T. N. and Khan, I. *Polym. Commun.* 1983, **24**, 162